https://doi.org/10.46861/bmp.31.001 PŮVODNÍ PRÁCE/ORIGINAL PAPER

Ammoniozippeite from the Jáchymov ore district, Krušné hory Mountains (Czech Republic) - description and Raman spectroscopy

Jiří Sejkora[1)]*, Zdeněk Dolníček[1)] and Jakub Plášil[2)]

[1)]*Department of Mineralogy and Petrology, National Museum, Cirkusová 1740, 193 00 Praha 9 - Horní Počernice; *e-mail: jiri.sejkora@nm.cz*

[2)]*Institute of Physics of the Czech Academy of Science, Na Slovance 1999/2, 182 21 Praha 8, Czech Republic*

Sejkora J, Dolníček Z, Plášil J (2023) Ammoniozippeite from the Jáchymov ore district, Krušné hory Mountains (Czech Republic) - description and Raman spectroscopy. Bull Mineral Petrolog 31(1): 1-9 ISSN 2570-7337

Abstract

We have undertaken a study of the rare ammonium uranyl sulphate mineral, ammoniozippeite, from the Jáchymov ore district, Krušné hory Mountains (Czech Republic). It has been found on a few specimens and forms rich crystalline aggregates in thin cracks of supergene altered rocks with uraninite veinlets in association with gypsum. Its radially arranged aggregates are composed by well-developed flattened acicular crystals up to 1 mm in length. Ammoniozippeite is bright yellow and locally even yellow-orange with pale yellow streak and fluoresces yellow, weak or dull under 254 nm and 366 nm UV-radiation, respectively. Ammoniozippeite crystals are transparent to translucent and have an intensive vitrous luster. It is a very brittle and at least one system of perfect cleavage (along {010}) was observed. The quantitative chemical analyses of ammoniozippeite agree well with the proposed ideal composition and correspond to the following empirical formula $[(NH_4)_{1.96}K_{0.11}]_{\Sigma 2.07}[(UO_2)_2(SO_4)_{1.98}O_{2.06}]\cdot H_2O$ (on the basis of 2 U atoms *pfu*). Ammoniozippeite is orthorhombic, the space group *Ccmb*, with the unit-cell parameters refined from X-ray powder diffraction data: *a* 8.7862(13), *b* 14.1579(19), *c* 17.162(2) Å and *V* 2134.8(4) Å^3. Vibrational (Raman and infrared) spectroscopy documented the presence molecular water, ammonium, uranyl and suphate units in the crystal structure of ammoniozippeite.

Key words: *ammoniozippeite, zippeite group, unit-cell parameters, chemical composition, Raman spectroscopy, infrared spectroscopy, Jáchymov, Czech Republic*

Received 10. 4. 2023; accepted 12. 6. 2023

Introduction

The discovery of the first yellow earthy uranyl sulfate, most probably of the zippeite group, was made by John (1821) during his study of uranium minerals from Jáchymov (St. Joachimsthal), Czech Republic. The mineral name zippeite was introduced later by Haidinger (1845), who applied it to the material studied by John. Despite recognition of zippeite almost one century ago, this uranyl sulfate remains poorly characterized. Until 1976, it was accepted that zippeite is a hydrated uranyl sulfate mineral with the uranium-to-sulfur molar ration equal to 2 devoid of cations. Frondel et al. (1976) analyzed natural and synthetic zippeite minerals, found contents of mono- and divalent cations and distinguished K, Na, Mg, Ni, Co and Zn end members. Details of the structures and chemistry of the zippeite-group minerals remained unknown.

Later, crystal structures of two synthetic members of zippeite group were published - zinczippeite (Spitsyn et al. 1982) and zippeite (Vochten et al. 1995). Burns et al. (2003) provided a complete crystallographic study based on the synthetic analogues of the zippeite-group minerals. Zippeites (mono- and divalent) are of monoclinic symmetry, mostly belonging to the *C*2/*m* space group (including those containing Mg^{2+}, Co^{2+}, Ni^{2+}, Zn^{2+} and one of the synthetic NH_4^+ zippeites), *C*2 (zippeite), $P2_1/n$ (natrozippeite), $P2_1/c$ (a second synthetic Mg^{2+} member) and orthorhombic *Cmca* (a second synthetic NH_4^+ zippeite).

Brugger et al. (2003) described a new Mg-dominant mineral species marécottite with triclinic symmetry (*P*-1) and zippeite-type sheets in the crystal structure and reported the redefinition of magnesiozippeite (*C*2/*m*); crystal structure of marécottite was refined by Plášil and Škoda (2015). Brugger et al. (2006) published crystal structure data for pseudojohannite, a new mineral species from Jáchymov (Ondruš et al. 2003c), and inferred its triclinic symmetry (*P*1 or *P*-1), later its crystal structure was refined in the space group *P*-1 by Plášil et al. (2012) and Plášil (2015). Peeters et al. (2008) reported crystallographic data for synthetic zippeites with mixed cationic site (K^+ with Mn^{2+}, Co^{2+}, Ni^{2+} and Zn^{2+}) and introduced the important idea that potassium content in zippeite can be variable.

In following years, Plášil et al. (2011b, 2013) determined crystal structure of natural zippeite (monoclinic *C*2/*m*) and magnesiozippeite (monoclinic *C*2/*m*); the first member with trivalent cation (Y^{3+}) was described by Plášil et al. (2011a) as a new mineral sejkoraite-(Y) (triclinic *P*-1); crystal structure of triclinic (*P*-1) Ca-dominant member, rabejacite, was solved (Plášil et al. 2014), the first K-Mn member was described by Plášil et al. (2017) as a new mineral plavnoite (monoclinic *C*2/*c*); the NH_4-Mn member was described as a new mineral redcanyonite by Olds et al. (2018); and finally Kampf et al. (2018) published as a new mineral, orthorhombic (*CCmb*) NH_4^+ dominant

member, ammoniozippeite. A short overview of members of the zippeite group is given in the Table 1. It should be noted that the zippeite group has not yet been formally approved by the CNMNC of IMA following the rule of Mills et al. (2009).

Ammoniozippeite was described by Kampf et al. (2018) as a new mineral from the Blue Lizard mine, San Juan Co. (Utah) and the Burro mine, San Miguel Co. (Colorado), both USA. Other its occurrences are reported (https://www.mindat.org/min-52182.html) from France

Table 1 *Overview of the symmetry, space group and ideal chemical formulae of the members of zippeite-group*

mineral	reference	ideal formula	symmetry	SG
zippeite	Plášil et al. (2011b)	$K_2[(UO_2)_4O_2(SO_4)_2(OH)_2](H_2O)_4$	monoclinic	*C*2/*m*
magnesiozippeite	Plášil et al. (2013)	$Mg[(UO_2)_2O_2(SO_4)](H_2O)_{3.5}$	monoclinic	*C*2/*m*
zinczippeite*	Burns et al. (2003)	$Zn[(UO_2)_2(SO_4)O_2](H_2O)_{3.5}$	monoclinic	*C*2/*m*
cobaltzippeite*	Burns et al. (2003)	$Co[(UO_2)_2(SO_4)O_2](H_2O)_{3.5}$	monoclinic	*C*2/*m*
redcanyonite	Olds et al. (2018)	$(NH_4)_2Mn[(UO_2)_4O_4(SO_4)_2](H_2O)_4$	monoclinic	*C*2/*m*
plavnoite	Plášil et al. (2017)	$K_{0.8}Mn_{0.6}[(UO_2)_2O_2(SO_4)]\cdot 3.5H_2O$	monoclinic	*C*2/*c*
natrozippeite*	Burns et al. (2003)	$Na_5[(UO_2)_8(SO_4)_4O_5(OH)_3](H_2O)_{12}$	monoclinic	$P2_1/n$
marécottite	Plášil, Škoda (2015)	$Mg_3[(UO_2)_4O_3(OH)(SO_4)_2]_2(H_2O)_{28}$	triclinic	*P*-1
pseudojohannite	Plášil (2015)	$Cu_3(OH)_2[(UO_2)_4O_4(SO_4)_2](H_2O)_{12}$	triclinic	*P*-1
sejkoraite-(Y)	Plášil et al. (2011a)	$Y_3(OH)_2[(UO_2)_8O_7OH(SO_4)_4](H_2O)_{24}$	triclinic	*P*-1
rabejacite	Plášil et al. (2014)	$Ca_2[(UO_2)_4O_4(SO_4)_2](H_2O)_8$	triclinic	*P*-1
ammoniozippeite	Kampf et al. (2018)	$(NH_4)_2[(UO_2)_2(SO_4)O_2]\cdot H_2O$	orthorhombic	*Ccmb*

Asterisks (*) at mineral name indicate data of synthetic analogues of natural members.

Fig. 1 *Rich crystalline aggregate of amonniozippeite in thin cracks of supergene altered rock from Jáchymov; field of view 4.2 mm; photo J. Sejkora.*

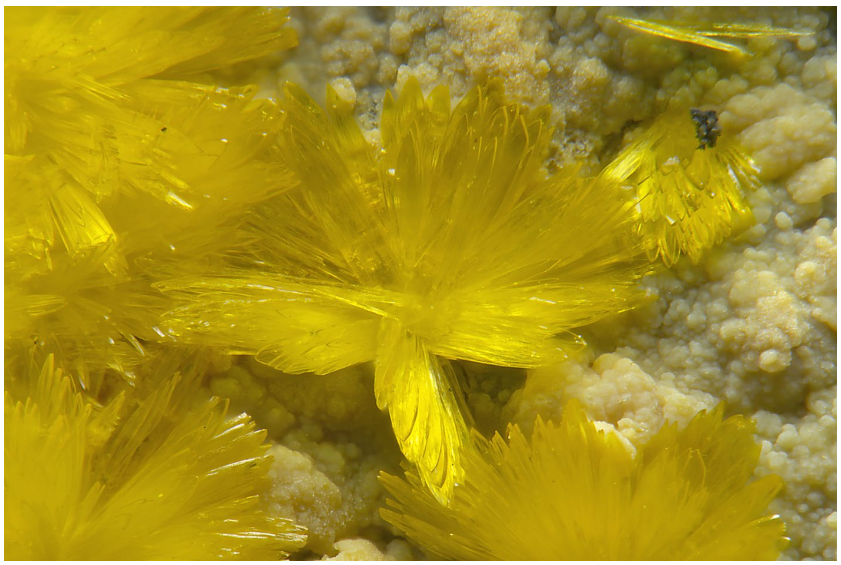

Fig. 2 *Radially arranged aggregate of flattened acicular crystals of ammoniozippeite from Jáchymov; field of view 2 mm; photo J. Sejkora.*

(Mas d´Alary), Germany (Menzenschwand, Kleinrückerwalde) and Hungary (Kövágószölös) but without any analytical data. This paper aims to summarize results of the complex mineralogical study including Raman and infrared spectroscopy of this rare ammonium uranyl sulfate mineral on the base of finds of well-crystallized samples in the Jáchymov ore district, Czech Republic.

Occurrence and specimen description

Ammoniozippeite was found on specimens originating from the Jáchymov ore district (formerly St. Joachimsthal), Krušné hory Mountains, approximately 20 km north of Karlovy Vary, northwestern Bohemia, Czech Republic. Material probably originates from the level 180 m of the Rovnost mine or the level 90 m of the Jiřina mine located in the central part of this ore district (Škácha et al. 2019).

The Jáchymov ore district is a classic example of Ag+As+Co+Ni+Bi and U vein-type hydrothermal mineralization. The ore veins cut a complex of medium-grade metasedimentary rocks of Cambrian to Ordovician age, in the envelope of a Variscan granite pluton. The majority of the ore minerals were deposited during the Variscan mineralizing epoch from mesothermal fluids (Ondruš et al. 2003a,b,d). Primary and supergene mineralization in this district resulted in extraordinarily varied associations; more than 440 mineral species have been reported from there (Ondruš et al. 1997a,b and 2003c,d; Hloušek et al. 2014; Škácha et al. 2019).

Ammoniozippeite has been found on a few specimens and forms rich crystalline aggregates (Fig. 1) in thin cracks of supergene altered rocks with uraninite veinlets in association with gypsum. Its radially arranged aggregates are composed by well-developed flattened acicular crystals up to 1 mm in length (Fig. 2). The mineral is bright yellow and locally even yellow-orange with pale yellow streak. Fluorescence of ammoniozippeite is yellow, weak or dull under 254 nm and 366 nm UV-radiation, respectively. Crystals are transparent to translucent and have an intensive vitrous luster. Mineral is very brittle and at least one system of perfect cleavage (probably along {010}) was observed.

Chemical composition

Samples of ammoniozippeite were analysed with a Cameca SX-100 electron microprobe (National Museum, Prague) operating in the wavelength-dispersive mode with an accelerating voltage of 15 kV, a specimen current of 5 nA, and a beam diameter of 20 μm. The following lines and standards were used: *K*α: BN (N), celestine (S), sanidine (K) and *M*α: UO_2 (U). Peak counting times (CT) were 200 s for nitrogen and 20 s for other elements; CT for each background was one-half of the peak time. The raw intensities were converted to the concentrations automatically using the *PAP* (Pouchou and Pichoir 1985) matrix-correction algorithm. The contents of Al, As, Ba, Bi, Ca, Cl, Co, Cr, Cu, Fe, Mg, Mn, Mo, Na, Ni, P, Pb, Si, Sr, V, Y and Zn were also measured, but always found to be below the detection limits (about 0.05 - 0.10 wt. %). The collected data were manually corrected for the partial overlap of the N*K*α peak with an unidentifiable U line (U N4-N6 according Kampf et al. 2018); pure UO_2 generated false content of 2.15 wt. % $(NH_4)_2O$. Overlap K*K*α - U*M*β1 was corrected automatically (standard UO_2, intensity 3.54 cps/nA). Water content could not be analysed directly because of the minute amount of material available. The H_2O content was confirmed by infrared spectroscopy and calculated by stoichiometry of ideal formula. The high totals could be result of H_2O loss under vacuum in the EPMA chamber.

Chemical composition of studied sample (Table 2) agrees very well with the ideal formula of ammoniozippeite $(NH_4)_2[(UO_2)_2(SO_4)O_2]\cdot H_2O$ and published analyses of this mineral phase from type localities (Kampf et al. 2018). The cationic sites are occupied by dominant NH_4^+ with minor contents of K (up to 0.13 *apfu*). The empirical formula of ammoniozippeite (mean of 11 analyses) on the basis of 2 U atoms *pfu* is $[(NH_4)_{1.96}K_{0.11}]_{\Sigma 2.07}[(UO_2)_2(SO_4)_{1.98}O_{2.06}]\cdot H_2O$. In comparison with the type material (Kampf et al. 2018), we observed slightly increased contents of K in ammoniozippeite from Jáchymov.

X-ray powder diffraction

Powder X-ray diffraction data were collected on a Bruker D8 Advance diffractometer (National Museum, Prague) with a solid-state 1D LynxEye detector using CuK_α radiation and operating at 40 kV and 40 mA. The powder pattern was collected using Bragg-Brentano geometry in the range 2.5 - 70° 2θ, in 0.01° steps with a counting time of 20 s per step. Positions and intensities of reflections were found and refined using the PearsonVII profile-shape function with the ZDS program package (Ondruš 1993) and the unit-cell parameters were refined by the least-squares algorithm implemented by Burnham (1962). The experimental powder pattern was indexed in line with the calculated values of intensities obtained from the crystal structure of ammoniozippeite (Kampf et al. 2018), based on Lazy Pulverix program (Yvon et al. 1977).

Table 2 *Chemical composition of ammoniozippeite (wt. %)*

	Jáchymov		Burro mine		Blue Lizard mine		ideal
	this paper		Kampf et al. (2018)		Kampf et al. (2018)		composition
	mean	range (n = 11)	mean	range (n = 5)	mean	range (n = 4)	
$(NH_4)_2O$	7.19	6.58 - 7.95	7.29	6.96 - 7.76	7.36	6.88 - 7.64	7.21
Na_2O			0.13	0.04 - 0.14	0.19	0.05 - 0.33	
K_2O	0.72	0.58 - 0.85			0.43	0.36 - 0.51	
SO_3	11.03	10.48 - 11.63	11.45	10.80 - 12.44	11.00	10.61 - 11.37	11.09
UO_3	80.64	78.18 - 82.23	81.10	79.24 - 84.24	81.90	79.69 - 85.04	79.21
H_2O*	2.54		2.56		2.56		2.49
total	102.11		102.53		103.44		100.00

H_2O* calculated on the base of ideal content of one water molecule *pfu*.

Table 3 *X-ray powder diffraction data of ammoniozippeite from Jáchymov*

d_{obs}	I_{obs}	d_{calc}	h	k	l	d_{obs}	I_{obs}	d_{calc}	h	k	l	d_{obs}	I_{obs}	d_{calc}	h	k	l
8.608	1.62	8.581	0	0	2	2.2247	0.67	2.2247	0	4	6	1.7158	0.14	1.7162	0	0	10
7.094	100.00	7.079	0	2	0	2.1966	0.22	2.1966	4	0	0	1.6977	0.34	1.6981	2	2	9
5.641	0.11	5.632	1	1	2	2.1448	0.22	2.1452	0	0	8	1.6907	0.17	1.6917	4	2	6
5.470	1.29	5.461	0	2	2	2.1408	0.17	2.1409	2	0	7	1.6675	0.14	1.6679	0	2	10
4.293	1.34	4.290	0	0	4	2.1281	0.06	2.1279	4	0	2	1.6343	0.14	1.6338	3	7	2
4.263	0.50	4.256	2	0	1	2.0979	0.20	2.0979	4	2	0	1.6073	0.11	1.6078	4	6	0
3.671	0.53	3.669	0	2	4	2.0654	0.25	2.0637	2	6	1	1.5777	0.20	1.5779	2	8	3
3.649	0.25	3.647	2	2	1	2.0503	0.25	2.0492	2	2	7	1.5681	0.11	1.5682	2	4	9
3.542	27.70	3.539	0	4	0	2.0368	0.11	2.0379	4	2	2	1.5631	0.08	1.5631	4	4	6
3.486	1.32	3.484	2	0	3	1.9538	0.53	1.9538	2	6	3	1.5456	0.11	1.5442	0	4	10
3.274	0.76	3.272	0	4	2	1.8661	0.20	1.8664	4	4	0	1.5427	0.08	1.5422	1	9	1
3.128	1.54	3.126	2	2	3	1.8324	0.08	1.8318	2	4	7	1.5342	0.31	1.5361	1	7	7
2.861	3.50	2.860	0	0	6	1.8241	0.11	1.8237	4	4	2	1.5050	0.14	1.5050	0	8	6
2.732	0.17	2.730	0	4	4	1.8201	0.31	1.8202	0	6	6	1.4296	0.17	1.4290	6	2	1
2.723	0.17	2.721	2	4	1	1.7697	1.57	1.7697	0	8	0	1.4178	0.08	1.4186	6	0	3
2.653	1.26	2.652	0	2	6	1.7490	0.31	1.7492	2	0	9	1.4155	0.14	1.4158	0	10	0
2.4833	0.50	2.4830	2	4	3	1.7434	0.11	1.7421	4	0	6	1.4047	0.08	1.4052	2	6	9
2.3601	4.00	2.3597	0	6	0	1.7338	0.20	1.7333	0	8	2	1.4013	0.17	1.4015	4	6	6

Table 4 *Unit-cell parameters for ammoniozippeite (for orthorhombic space group Ccmb)*

		a [Å]	b [Å]	c [Å]	V [Å^3]
Jáchymov	this paper	8.7862(13)	14.1579(19)	17.162(2)	2134.8(4)
Burro mine[1]	Kampf et al. (2018)	8.7944(3)	14.3296(7)	17.1718(12)	2164.0(2)
Burro mine[2]	Kampf et al. (2018)	8.812(3)	14.351(5)	17.204(5)	2175.6(12)
synthetic[3]	Burns et al. (2003)	8.7748(5)	14.2520(9)	17.1863(10)	2149.3(2)

Burro mine[1] - single crystal data; Burro mine[2] - X-ray powder diffraction data; synthetic[3] SZIPPNH4II with ideal formula $(NH_4)_2[(UO_2)_2(SO_4)O_2]$.

The peak positions in experimental X-ray powder patterns (Table 3) agree well with data published for ammoniozippeite from type locality (Kampf et al. 2018) as well as with those calculated from the crystal structure of this mineral. The observed significant differences in intensities of individual diffraction maxima are due by the by strong preferred orientation effects due to {010} perfect cleavage. The refined unit-cell parameters, compared with published data, are given in the Table 4.

Raman spectroscopy

The Raman spectra of studied sample were collected in the range 4000 - 50 cm^{-1} using a DXR dispersive Raman Spectrometer (Thermo Scientific) mounted on a confocal Olympus microscope. The Raman signal was excited by an unpolarised red 633 nm He-Ne gas laser and detected by a CCD detector. The experimental parameters were: 50x objective, 10 s exposure time, 100 exposures, 25 μm pinhole spectrograph aperture and 8 mW laser power level. The spectra were repeatedly acquired from different grains in order to obtain a representative spectrum with the best signal-to-noise ratio. The eventual thermal damage of the measured point was excluded by visual inspection of excited surface after measurement, by observation of possible decay of spectral features in the start of excitation and checking for thermal downshift of Raman lines. The instrument was set up by a software-controlled calibration procedure using multiple neon emission lines (wavelength calibration), multiple polystyrene Raman bands (laser-frequency calibration) and standardized white-light sources (intensity calibration).

Spectral manipulations were performed using the Omnic 9 software (Thermo Scientific). Gaussian/Lorentzian (pseudo-Voigt) profile functions of the band-shape were used to obtain decomposed band components of the spectra. The decomposition was based on the minimization of the difference in the observed and calculated profiles until the squared correlation coefficient (r^2) was greater than 0.995.

Ammoniozippeite, $(NH_4)_2[(UO_2)_2(SO_4)O_2]\cdot H_2O$, is an orthorhombic uranyl-containing mineral, the space group *Ccmb*, Z = 8. In the asymmetric part of the unit cell, there are one U site, occupied by U^{6+}, one S site, occupied by S^{6+} and three symmetrically independent sites occupied by two NH_4^+ groups and one water molecule bonded by hydrogen bonds. The crystal structure of ammoniozippeite contains edge-sharing zig-zag chains of UO_7 pentagonal bipyramids linked by sharing corners with $(SO_4)^{2-}$ groups, yielding a $[(UO_2)_2(SO_4)O_2]^{2-}$ sheet based on the zippeite-type topology. The interlayer region contains two NH_4^+ groups and one H_2O group, statistically distributed over three sites (Kampf et al. 2018).

Molecular water (C_{2v} symmetry) is characterized by three fundamental ν_1 (A_1) symmetric stretching OH vibrations (~3657 cm^{-1}), ν_2 (δ H_2O) (A_1) bending vibrations (~1595 cm^{-1}) and ν_3 (B_1) antisymmetric stretching OH (~3756 cm^{-1}) vibrations. All vibrations are Raman and infrared active. Their wavenumbers are influenced by formation of hydrogen bonds. At wavenumbers lower than 1100 cm^{-1}, libration modes of water molecules may be observed (Čejka 1999; Nakamoto 2009). A free tetrahedral ammonium group, NH_4^+ (T_d symmetry) is characterized by four normal vibration modes (Nakamoto 2009): the ν_1 symmetric stretching vibration, Raman active (~3040 cm^{-1}),

the ν_2 doubly degenerate bending vibration, Raman active (~1680 cm^{-1}), the ν_3 triply degenerate stretching vibration, Raman and infrared active (~3145 cm^{-1}) and ν_4 triply degenerate bending vibration, Raman and infrared active (~1400 cm^{-1}).

A free uranyl cation, $(UO_2)^{2+}$, $D_{\infty h}$ point-group symmetry, is, in general, characterized by three fundamental vibration modes: the ν_1 symmetric stretching vibration, Raman active (900 - 750 cm^{-1}), the ν_2 (δ) doubly degenerate bending vibration, infrared active (300 - 200 cm^{-1}),

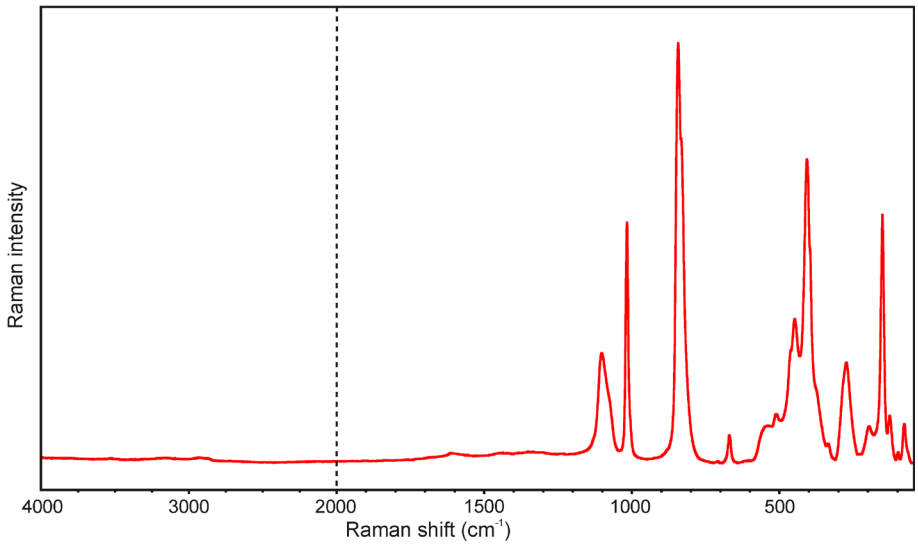

Fig. 3 *Raman spectrum for ammoniozippeite from Jáchymov (split at 2000 cm^{-1}).*

Table 5 *Tentative assignment of Raman spectrum of ammoniozippeite from Jáchymov*

position	*FWHH*	$I_{rel.}$	$I_{rel.}$	*Burro mine**		*tentative assignment*
[cm^{-1}]	[cm^{-1}]	height	area	[cm^{-1}]		
3529	47	0.2	0.3			ν O-H stretch of hydrogen bonded water molecules
3158	201	0.7	4.0			ν O-H stretch of hydrogen bonded water molecules;
2918	139	1.1	6.0			ν_1, ν_3 N-H stretch of NH_4^+ groups
1604	85	1.8	8.3			ν_2 bend of hydrogen bonded water molecules
1446	58	0.9	1.7			ν_4 bend of NH_4^+ groups
1345	115	1.1	3.6	1390	w	
1101	29	33.6	34.0	1120	vw	ν_3 antisymmetric stretch of $(SO_4)^{2-}$
1077	26	14.4	12.8	1098	vw	
1016	9	80.3	25.4	1013	m	ν_1 symmetric stretch of $(SO_4)^{2-}$
1005	11	7.2	2.7			
845	13	96.0	39.7	846	m	ν_1 symmetric stretch of $(UO_2)^{2+}$
831	25	98.1	91.7	826	vs	
				806	m	
669	12	9.6	4.0	664	vw	ν_4 bend of $(SO_4)^{2-}$
				608	vw	
553	41	10.2	14.2			libration mode of H_2O
508	55	13.6	26.2	508	w	
465	23	16.5	14.1	461	m	ν_2 bend of $(SO_4)^{2-}$
446	27	35.8	36.6			
406	24	100.0	100.0	406	s	
394	6	13.9	2.8			
370	33	12.5	14.4	368	w	
333	12	3.5	1.4	327	w	$\nu_{rotational}$ of NH_4^+ groups
288	13	3.5	1.6	283	w	ν_2 bend of $(UO_2)^{2+}$
273	38	38.6	56.0	268	w	
				213	m	lattice and other modes
196	35	13.3	17.0	203	m	
162	27	8.5	8.0			
150	12	79.2	33.6	148	s	
125	16	14.7	7.9			
98	9	3.6	1.1			
77	11	13.6	5.3			
65	14	3.4	1.7			

$I_{rel.}$ calculated from peak height and band area; * Kampf et al. (2018).

and the ν_3 antisymmetric stretching vibrations, infrared active (1000 - 850 cm^{-1}). The lowering of the ideal symmetry (due to crystal field and so on) may cause splitting of the ν_2 (δ) vibration and Raman and infrared activation of all three vibrations (Čejka 1999; Nakamoto 2009). A free sulphate anion, $(SO_4)^{2-}$, T_d point-group symmetry, is characterized by four fundamental modes: the ν_1 symmetric stretching vibration, Raman active (~983 cm^{-1}), the ν_2 (δ) doubly degenerate bending vibration, Raman active (~450 cm^{-1}), the ν_3 triply degenerate antisymmetric stretching vibration, Raman and infrared active, (~1105 cm^{-1}), and the ν_4 (δ) triply degenerate bending vibration, Raman and infrared active (~611 cm^{-1}). T_d symmetry lowering may cause splitting of degenerate vibrations and Raman and infrared activation of all vibrations (Čejka 1999; Nakamoto 2009).

The Raman spectrum of ammoniozippeite sample from Jáchymov, recently studied, is close to the published spectrum of ammoniozippeite from Burro Mine (Kampf et al. 2018). Our new Raman spectrum, however, offers a better resolution and includes also the region of vibrations of water molecules.

The full-range Raman spectrum of the studied mineral ammoniozippeite is given in Figure 3 and wavenumbers with assignments are given in Table 5. Bands of the very low intensity, located at 3529, 3158 and 2918 cm^{-1} (Fig. 4a), are connected with the ν OH stretching vibrations of hydrogen-bonded water molecules; bands at 3158 and 2918 cm^{-1} along with ν_1 and ν_3 N-H stretching vibration from interlayer NH_4^+ groups. According to the empirical relation between energy of vibration and the corresponding bond length (Libowitzky 1999), O-H×××O hydrogen-bond lengths vary approximately in the range from 2.63 to

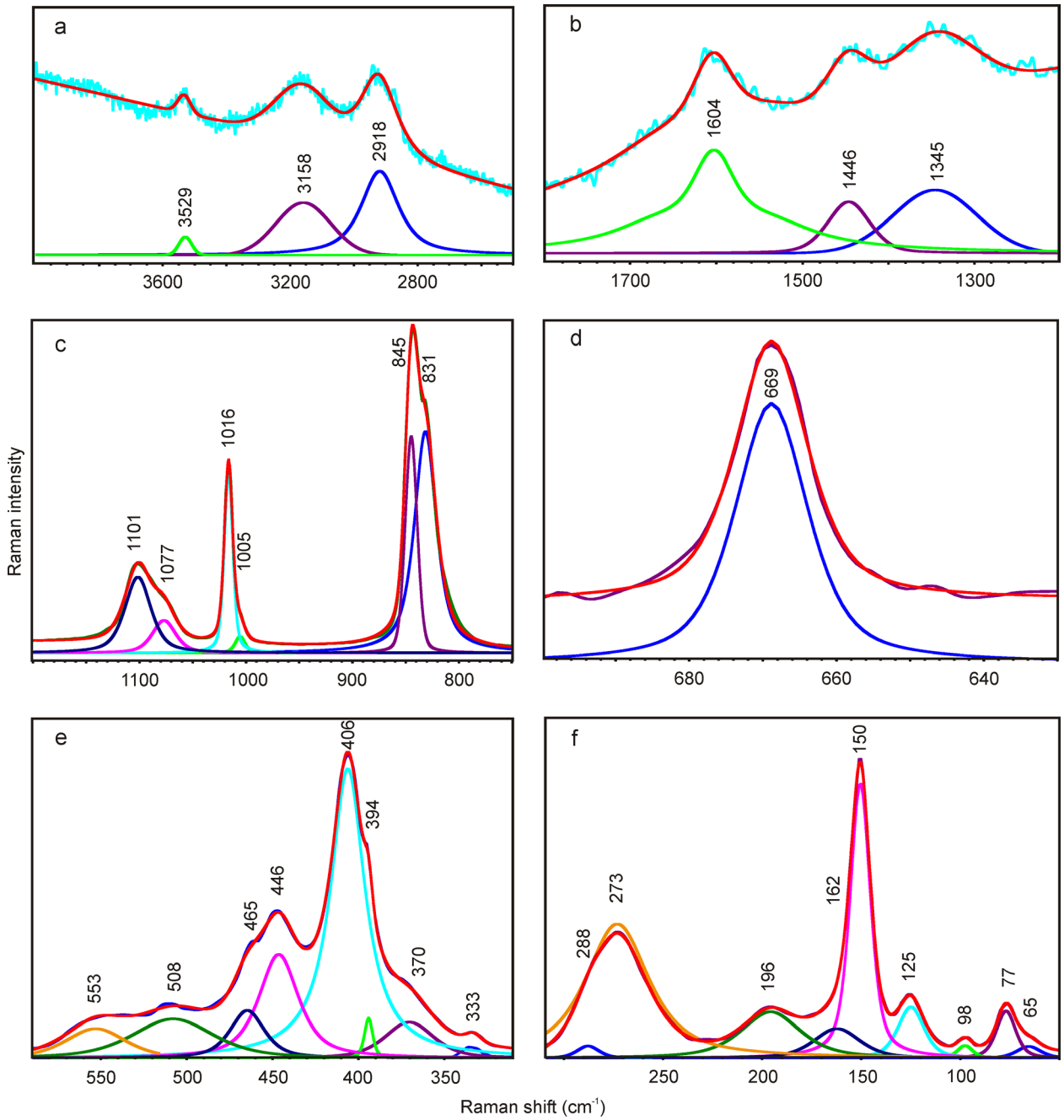

Fig. 4 *Results of the band component analysis in the Raman spectrum of ammoniozippeite from Jáchymov: a) 4000 - 2500 cm^{-1}; b) 1800 - 1200 cm^{-1}; c) 1200 - 750 cm^{-1}; d) 700 - 630 cm^{-1}; e) 590 - 310 cm^{-1}; f) 310 - 50 cm^{-1}.*

2.95 Å. A very weak band at 1604 cm^{-1} (Fig. 4b) is attributed to the ν_2 bending vibrations of water molecules. Very weak and broad bands at 1146 and 1345 cm^{-1} (Fig. 4b) are related to the ν_4 bending vibration of NH_4^+ groups.

A medium-intensity band with two components at 1101 and 1077 cm^{-1} (Fig.4c) is assigned to the split triply degenerate ν_3 $(SO_4)^{2-}$ antisymmetric stretching vibrations. A strong band at 1016 cm^{-1} with shoulder at 1005 cm^{-1} (Fig. 4c) are attributed to the ν_1 $(SO_4)^{2-}$ symmetric stretching vibrations. Very strong band with component at 845 and 831 cm^{-1} (Fig. 4c) is assigned to the ν_1 $(UO_2)^{2+}$ symmetric stretching vibrations, corresponding to U-O bond lengths in uranyl 1.77 - 1.78 Å (Bartlett, Cooney 1989). The inferred U-O bond lengths for the uranyl ion are comparable with data derived from the X-ray studies for ammoniozppeite (1.778 - 1.786 Å, Kampf et al. 2018).

A weak band at 669 cm^{-1} (Fig. 4d) is connected with the split triply degenerate ν_4 (δ) $(SO_4)^{2-}$ bending vibrations. Weak and broad bands at 553 and 508 cm^{-1} (Fig. 4e) may be connected with the libration mode of water molecules. Medium-strong and strong bands at 446 and 406 cm^{-1} with shoulders at 465, 394 and 370 cm^{-1} (Fig. 4e) are assigned to the split doubly degenerate ν_2 $(SO_4)^{2-}$ bending vibrations; a weak band at 333 cm^{-1} (Fig. 4e) may be associated with $\nu_{rotational}$ of NH_4^+ group in interlayer (Heyns et al. 1987).

A medium-intensity band with two components at 288 and 273 cm^{-1} (Fig. 4f) is related to the ν_2 $(UO_2)^{2+}$ doubly degenerate bending vibrations. A strong band at 150 cm^{-1} and weak bands at 162, 125, 98, 77 and 65 cm^{-1} (Fig. 4f) may be attributed to O_{eq}-U-O_{eq} bending vibrations (Ohwada 1976), U-O_{eq}-ligand stretching modes (Bullock, Paret 1970; Ohwada 1976; Plášil et al. 2010), $\nu_{translational}$ of NH_4^+ groups (Heyns et al. 1987), UO_2^{2+} translations and rotations and external lattice vibration modes (Plášil et al. 2010; Kampf et al. 2018).

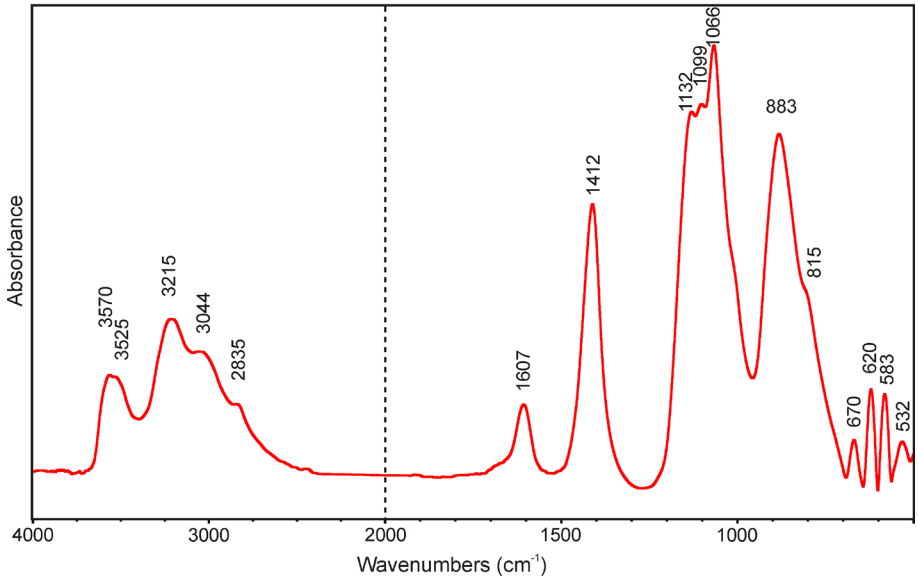

Fig. 5 *Infrared spectrum for ammoniozippeite from Jáchymov (split at 2000 cm^{-1}).*

Table 6 *Tentative assignment of infrared spectrum of ammoniozippeite from Jáchymov*

position		*Burro mine**		*tentative assignment*
[cm^{-1}]		[cm^{-1}]		
3570	ms			ν O-H stretch of hydrogen bonded water molecules
3525	ms	~3525	ms	
3215	ms	~3190	vs	ν O-H stretch of hydrogen bonded water molecules; ν_3 N-H stretch of NH_4^+ groups
3044	ms	~3040	s	
2835	ms	~2700	ms	
1607	ms	1626	w	ν_2 bend of hydrogen bonded water molecules
1412	s	1408	vs	ν_4 bend of NH_4^+ groups
1132	s	1138	w	ν_3 antisymmetric stretch of $(SO_4)^{2-}$
1099	s	1120	s	
1066	vs	1065	s	
		1008	w	ν_1 symmetric stretch of $(SO_4)^{2-}$
		993	w	
883	vs	933	vs	ν_3 antisymmetric stretch of $(UO_2)^{2+}$
		846	ms	ν_1 symmetric stretch of $(UO_2)^{2+}$ and/or libration mode of H_2O
815	s	832	ms	
670	w			ν_4 bend of $(SO_4)^{2-}$
620	ms			
583	ms			libration mode of H_2O
532	w			

* Kampf et al. (2018).

Infrared spectroscopy

The infrared vibrational spectrum of ammoniozippeite was recorded by the attenuated total reflection (ATR) method with a diamond cell on a Nicolet iS5 spectrometer. Spectra over the 4000 - 400 cm^{-1} range were obtained by the co-addition of 64 scans with a resolution of 4 cm^{-1} and a mirror velocity of 0.4747 cm/s. Spectra were co-added to improve the signal-to-noise ratio.

Infrared spectra of ammoniozippeite from Blue Lizard mine and Burro mine (both USA) were recently published by Kampf et al. (2018); our experimental spectrum of sample from Jáchymov is very similar especially to published spectrum for sample from Blue Lizard mine. The full-range spectrum is given in Figure 5 and its tentative assignment in Table 6. Strong and broad infrared bands at 3570, 3525, 3215, 3044 and 2835 cm^{-1} are assigned to the ν O-H stretching vibration of hydrogen bonded water molecules, part of these bands between 3300 - 2600 cm^{-1} also to ν_3 N-H stretching vibrations of NH_4^+ group. According to Libowitzky (1999) correlation function, O-H×××O hydrogen bond lengths vary approximately from 3.1 to 2.6 Å. A medium infrared band at 1607 cm^{-1} is attributed to the ν_2 H_2O bending vibration of water molecules and strong band at 1412 cm^{-1} to ν_4 bending vibration of NH_4^+ groups in the interlayer.

Infrared bands at 1132, 1099 and 1066 cm^{-1} are assigned to the split triply degenerate ν_3 $(SO_4)^{2-}$ antisymmetric stretching vibrations. We do not obseved bands corresponding to the ν_1 $(SO_4)^{2-}$ symmetric stretching vibration; Kampf et al. (2018) stated for sample from Burro mine weak bands at 1008 and 993 cm^{-1}. Strong infrared band at 883 cm^{-1} with shoulder at 815 cm^{-1} are attributed to ν_3 $(UO_2)^{2+}$ antisymmetric and ν_1 $(UO_2)^{2+}$ symmetric stretching vibrations, respectively. Coincidences with the libration mode of H_2O molecules are also possible around 830 cm^{-1} (Kampf et al. 2018). Calculated uranyl U-O bond lengths using the empirical relation given by Bartlett, Cooney (1989) 1.797 (ν_3) and 1.796 (ν_1) Å are comparable with bond lengths 1.778 - 1.786 Å measured from the X-ray data (Kampf et al. 2018). Weak and medium strong bands at 670 and 620 cm^{-1} are connected with the split triply degenerate ν_4 $(SO_4)^{2-}$ bending vibrations. Medium strong and weak bands at 583 and 532 cm^{-1} may be connected with the libration mode of water molecules.

Conclusion

Very rare member of zippeite-group minerals, ammoniozippeite, was determined in the material from the Jáchymov ore district (Czech Republic) by X-ray powder diffraction and electron microprobe analyses. Molecular structure of this well-defined sample can be better constrained using the vibrational spectroscopy. Raman and infrared spectroscopy confirmed the presence of molecular water, ammonium, uranyl and suphate units in its crystal structure.

Acknowledgements

The study was financially supported by the Ministry of Culture of the Czech Republic (long-term project DKRVO 2019-2023/1.II.e; National Museum, 00023272).

References

Bartlett JR, Cooney RP (1989) On the determination of uranium-oxygen bond lengths in dioxouranium(VI) compounds by Raman spectroscopy. J Mol Struct 193: 295-300

Brugger J, Burns PC, Meisser N (2003) Contribution to the mineralogy of acid drainage of uranium minerals: marécottite and the zippeite group. Am Mineral 88: 676-685

Brugger J, Wallwork KS, Meisser N, Pring A, Ondruš P, Čejka J (2006) Pseudojohannite from Jáchymov, Musonoï, and La Creusaz: a new member of the zippeite-group. Am Mineral 91: 929-936

Bullock H, Parret FW (1970) The low frequency infrared and Raman spectroscopic studies of some uranyl complexes: the deformation frequency of the uranyl ion. Can J Chem 48: 3095-3097

Burnham Ch W (1962) Lattice constant refinement. Carnegie Inst Washington Year Book 61: 132-135

Burns PC, Deely KM, Hayden LA (2003) The crystal chemistry of the zippeite group. Can Mineral 41(3): 687-706

Čejka J (1999) Infrared spectroscopy and thermal analysis of the uranyl minerals. Rev Mineral 38: 521-622

Frondel C, Ito J, Honea RM, Weeks AM (1976) Mineralogy of the zippeite-group. Can Mineral 14: 429-436

Haidinger W (1845) Handbuch der bestimmenden Mineralogie. Wien

Heyns AM, Venter MW, Range KJ (1987) The vibrational spectra of NH_4VO_3 at elevated temperatures and pressures. Zeit Naturforsch B, 42(7): 843-852

Hloušek J, Plášil J, Sejkora J, Škácha P (2014) News and new minerals from Jáchymov, Czech Republic (2003 - 2014). Bull mineral-petrolog Odd Nár Muz (Praha) 22: 155-181

John JF (1821) Chemische untersuchung eines natürlichen Uranvitriols. Chem Untersuch 5: 254; Chem Phys 32: 248

Kampf AR, Plášil J, Olds TA, Nash BP, Marty J (2018) Ammoniozippeite, a new uranyl sulfate mineral from the Blue Lizard Mine, San Juan County, Utah, and the Burro Mine, San Miguel County, Colorado, USA. Can Mineral 56: 235-245

Libowitzky E (1999) Correlation of O-H stretching frequencies and O-H×××O hydrogen bond lengths in minerals. Monat Chem 130: 1047-1059

Mills SJ, Hatert F, Nickel EH, Ferraris G (2009) The standardisation of mineral group hierarchies: application to recent nomenclature proposals. Eur J Mineral 21: 1073-1080

Nakamoto K (2009) Infrared and Raman spectra of inorganic and coordination compounds Part A: Theory and applications in inorganic chemistry. John Wiley and Sons Inc. Hoboken, New Jersey

Ohwada K (1976) Infrared spectroscopic studies of some uranyl nitrate complexes. J Coord Chem 6: 75-80

Olds TA, Plášil J, Kampf AR, Burns PC, Nash BP, MartyJ, Rose TP, Carlson SM (2018) Redcanyonite, $(NH_4)_2Mn[(UO_2)_4O_4(SO_4)_2](H_2O)_4$, a new zippeite-group mineral from the Blue Lizard mine, San Juan County, Utah, USA. Mineral Mag 82(6): 1261-1275

Ondruš P (1993) ZDS - A computer program for analysis of X-ray powder diffraction patterns. Materials Science Forum, 133-136, 297-300, EPDIC-2. Enchede.

Ondruš P, Veselovský F, Hloušek J, Skála R, Frýda J, Čejka J, Gabašová A (1997a) Secondary minerals of the Jáchymov (Joachimsthal) ore district. J Czech Geol Soc 42: 3-76

Ondruš P, Veselovský F, Skála R, Císařová I, Hloušek J, Frýda J, Vavřín I, Čejka J, Gabašová A (1997b) New naturally occurring phases of secondary origin from Jáchymov (Joachimsthal). J Czech Geol Soc 42: 77-107

Ondruš P, Veselovský F, Gabašová A, Drábek M, Dobeš P, Malý K, Hloušek J, Sejkora J (2003a) Ore-forming processes and mineral parageneses of the Jáchymov ore district. J Czech Geol Soc 48: 157-192

Ondruš P, Veselovský F, Gabašová A, Hloušek J, Šrein V (2003b) Geology and hydrothermal vein system of the Jáchymov (Joachimsthal) ore district. J Czech Geol Soc 48: 3-18

Ondruš P, Veselovský F, Gabašová A, Hloušek J, Šrein V (2003c) Supplement to secondary and rock-forming minerals of the Jáchymov ore district. J Czech Geol Soc 48: 149-155

Ondruš P, Veselovský F, Gabašová A, Hloušek J, Šrein V, Vavřín I, Skála R, Sejkora J, Drábek M (2003d) Primary minerals of the Jáchymov ore district. J Czech Geol Soc 48: 19-147

Peeters OM, Vochten R, Blaton N (2008) The crystal structures of synthetic potassium - transition-metal zippeite-group phases. Can Mineral 46: 173-182

Plášil J (2015) Crystal structure refinement of pseudojohannite, $Cu_3(OH)_2[(UO_2)_4O_4(SO_4)_2](H_2O)_{12}$, from the type locality-Jachymov, Czech Republic. J Geosci 60(2): 123-127

Plášil J, Škoda R (2015) New crystal-chemical data for marécottite. Mineral Mag 79(3): 649-660

Plášil J, Buixaderas E, Čejka J, Sejkora J, Jehlička J, Novák M (2010) Raman spectroscopic study of the uranyl sulphate mineral zippeite: low wavenumber and U-O stretching regions. Anal Bioanal Chem 397: 2703-2715

Plášil J, Dušek M, Novák M, Čejka J, Císařová I, Škoda R (2011a) Sejkoraite-(Y), a new member of the zippeite group containing trivalent cations from Jáchymov (St. Joachimsthal), Czech Republic: description and crystal structure refinement. Am Mineral 96(7): 983-991

Plášil J, Mills SJ, Fejfarová K, Dušek M, Novák M, Škoda R, Čejka J, Sejkora J (2011b) The crystal structure of natural zippeite, $K_{1.85}H^+_{0.15}[(UO_2)_4O_2(SO_4)_2(OH)_2](H_2O)_4$, from Jáchymov, Czech Republic. Can Mineral 49(4): 1089-1103

Plášil J, Fejfarová K, Wallwork KS, Dušek M, Škoda R, Sejkora J, Čejka J, Veselovský F, Hloušek J, Meisser N, Brugger J (2012) Crystal structure of pseudojohannite, with a revised formula, $Cu_3(OH)_2[(UO_2)_4O_4(SO_4)_2](H_2O)_{12}$. Am Mineral 97: 1796-1803

Plášil J, Fejfarová K, Škoda R, Dušek M, Marty J, Čejka J (2013) The crystal structure of magnesiozippeite, $Mg[(UO_2)_2O_2(SO_4)](H_2O)_{3.5}$, from East Saddle Mine, San Juan County, Utah (U.S.A.). Mineral Petrol 107: 211-219

Plášil J, Dušek M, Čejka J, Sejkora J (2014) The crystal structure of rabejacite, the Ca^{2+}-dominant member of the zippeite group. Mineral Mag 78(5): 1249-1264

Plášil J, Škácha P, Sejkora J, Kampf AR, Škoda R, Čejka J, Hloušek J, Kasatkin AV, Pavlíček R, Babka K (2017) Plavnoite, a new K-Mn member of the zippeite group from Jáchymov, Czech Republic. Eur J Mineral 29(1): 117-128

Pouchou J, Pichoir F (1985) „PAP" (φρz) procedure for improved quantitative microanalysis. In: Armstrong JT (ed): Microbeam Analysis: 104-106. San Francisco Press. San Francisco

Škácha P, Plášil J, Horák V (2019) Jáchymov: mineralogická perla Krušnohoří. Academia, Praha 682 pp.

Spitsyn VI, Kovba LM, Tabachenko VV, Tabachenko NV, Mikhailov YuN (1982) Structure of the basic uranyl salts and polyuranates. Russ Chem Bull 31: 711-714

Vochten R, Van Haverbeke L, Van Springel K, Blaton N, Peeters OM (1995) The structure and physicochemical characteristics of synthetic zippeite. Can Mineral 33: 1091-1101

Yvon K, Jeitschko W, Parthé E (1977) Lazy Pulverix, a computer program for calculation X-ray and neutron diffraction powder patterns. J Appl Cryst 10: 73-74